



Published in final edited form as:

*Life Sci Space Res (Amst)*. 2020 August ; 26: 62–68. doi:10.1016/j.lssr.2020.04.002.

## Effects of single-dose protons or oxygen ions on function and structure of the cardiovascular system in male Long Evans rats

Vijayalakshmi Sridharan<sup>1,\*</sup>, John W Seawright<sup>2,\*</sup>, Reid D Landes<sup>3</sup>, Maohua Cao<sup>4</sup>, Preeti Singh<sup>1</sup>, Catherine M Davis<sup>5</sup>, Xiao-Wen Mao<sup>6</sup>, Sharda P Singh<sup>7</sup>, Xin Zhang<sup>8</sup>, Gregory A Nelson<sup>6</sup>, Marjan Boerma<sup>1</sup>

<sup>1</sup>Division of Radiation Health, University of Arkansas for Medical Sciences, Little Rock, AR

<sup>2</sup>McLennan Community College, Waco, TX, formerly at the Division of Radiation Health, University of Arkansas for Medical Sciences, Little Rock, AR

<sup>3</sup>Department of Biostatistics, University of Arkansas for Medical Sciences, Little Rock, AR

<sup>4</sup>College of Dentistry, Texas A&M University, Dallas, TX; formerly at the Division of Radiation Health, University of Arkansas for Medical Sciences, Little Rock, AR

<sup>5</sup>Department of Psychiatry and Behavioral Sciences, Johns Hopkins University School of Medicine, Baltimore, MD

<sup>6</sup>Department of Basic Sciences and Radiation Medicine, Loma Linda University, Loma Linda, CA

<sup>7</sup>Department of Internal Medicine, Texas Tech University Health Sciences Center, Lubbock, TX

<sup>8</sup>Department of Pharmacodynamics, University of Florida at Gainesville, Gainesville, FL.

### Abstract

**Purpose:** Studies are required to determine whether exposures to radiation encountered during manned missions in deep space may have adverse effects on the cardiovascular system. Most of the prior studies on effects of simulated space radiation on the heart and vasculature have been performed in mouse models. To provide data from a second animal species, two studies were performed to assess effects of high-energy charged particle radiation on the heart and abdominal aorta in a rat model.

**Materials and methods:** In study A, male Long Evans rats were exposed to whole-body protons (250 MeV, 0.5 Gy) or oxygen ions (<sup>16</sup>O, 600 MeV/n, 0.5 Gy), and ultrasonography was used to measure *in vivo* cardiac function and blood flow parameters at 3, 5, 9 and 12 months after radiation, followed by tissue collection at 12 months. In study B, male Long Evans rats were

---

**Address correspondence to:** Marjan Boerma, Ph.D., Division of Radiation Health, Department of Pharmaceutical Sciences, University of Arkansas for Medical Sciences, 4301 West Markham Slot 522-10, Little Rock, AR 72205, Phone: 501-686-6599, fax: 501-686-6057, mboerma@uams.edu.

\*These authors made equal contributions

**Publisher's Disclaimer:** sThis is a PDF file of an unedited manuscript that has been accepted for publication. As a service to our customers we are providing this early version of the manuscript. The manuscript will undergo copyediting, typesetting, and review of the resulting proof before it is published in its final form. Please note that during the production process errors may be discovered which could affect the content, and all legal disclaimers that apply to the journal pertain.

Disclosure statement

The authors report no conflicts of interest.

exposed to  $^{16}\text{O}$  (1 GeV/n, 0.01–0.25 Gy), and hearts collected at 6 to 7 and 12 months for histology and western-blot.

**Results:** Both protons (250 MeV) and  $^{16}\text{O}$  (600 MeV/n) caused a decrease in left ventricular posterior wall thickness at 3–5 months, but did not change echocardiographic measures of cardiac function. In Pulsed-wave Doppler assessment of the abdominal aorta, an increase was seen in mean velocity, peak velocity, and velocity time integral at 12 months after  $^{16}\text{O}$  (600 MeV/n), suggesting a change in vascular function. There were no significant changes in histopathology or histological quantification of total collagens in heart or aorta. On the other hand, an increase was seen in a 75 kDa peptide of collagen type III in the left ventricle of rats exposed to protons (250 MeV) and  $^{16}\text{O}$  (600 MeV/n and 1 GeV/n), suggesting that radiation caused remodeling of existing collagens in the heart.  $^{16}\text{O}$  (600 MeV/n and 1 GeV/n) caused increases in left ventricular protein levels of immune cell markers CD2, CD4, CD8, and CD68.

**Conclusion:** A single low dose of whole body protons or  $^{16}\text{O}$  in male Long Evans rats did not change cardiac function or induce gross pathological changes in the heart or aorta, but induced mild changes in vascular function and remodeling of existing collagens in the heart. Altogether, studies in prior mouse models and the current work in rats indicate minor changes in cardiac function and structure after a low dose of single-ion radiation.

## Keywords

space radiation; oxygen ions; protons; cardiovascular system; degenerative tissue effects

---

## 1. Introduction

For many years, studies have identified an increased rate of cardiovascular disease in human populations several decades after exposure to low doses of low-linear energy transfer (LET) radiation (1–5). Astronauts traveling beyond low Earth orbit such as on missions to Mars, a near-earth asteroid, or prolonged stays on the Moon, will be exposed to low doses of high-LET cosmic radiation (6). A full mission to Mars with return to Earth is expected to lead to exposures to cosmic radiation at total doses up to about 400 mGy (7,8).

Studies have begun to assess the potential cardiovascular effects of low-dose high-LET radiation exposures. Most of these studies have been performed in mouse models, providing evidence for changes in cardiac function and structure (9,10), increased cardiac expression of protein markers of immune cells (10,11) and cytokines (12), and changes in gene networks in cardiomyocytes (13,14) after both protons and heavy ions.

Since preclinical research performed in multiple animal species may enhance the translatability of the results to human subjects, we may investigate effects of simulated space radiation in animal species other than mouse. Some prior studies have been performed in rat models. Exposure to iron ions ( $^{56}\text{Fe}$  (1 GeV/n)) at doses of 0.5 and 1 Gy were shown to cause endothelial dysfunction and increase aortic stiffness in male Wistar rats (15). However, other cardiovascular effects of high-energy charged particles in rat models have not yet been explored as extensively as in the mouse.

Our main goal was to characterize cardiovascular function and structure in a rat model of exposure to low-dose high-LET radiation, relative to sham-irradiation, to strengthen prior findings from mouse models. For this purpose, we selected male rats of the Long Evans strain, an outbred strain regularly used in the study of the biological response to space radiation (16–19). Fragmentation of heavy ions in the wall of a space craft will lead to a radiation environment inside the craft that consists for a large part of ions of atomic number 10 (20). Therefore, to model radiation exposure during deep space missions, we used rats exposed to protons (250 MeV) or oxygen ions ( $^{16}\text{O}$ , 600 MeV/n and 1 GeV/n) in two separate studies. Ultrasonography was used to assess cardiac function and abdominal aorta blood flow in study A. Tissue samples of heart and abdominal aorta were collected to investigate pathological changes in both studies A and B, as outlined below.

## 2. Materials and Methods

Data were obtained from studies A and B. In short, in study A, male Long Evans rats were exposed to protons (250 MeV, 0.5 Gy) or  $^{16}\text{O}$  (600 MeV/n, 0.5 Gy), transported to the University of Arkansas for Medical Sciences (UAMS) and housed for 12 months after irradiation. Ultrasonography was used to measure *in vivo* cardiac function and blood flow parameters, and at 12 months, heart and abdominal aorta were collected for histology and western-blots. In addition, in a tissue sharing approach, hearts were obtained from study B that was performed at Johns Hopkins University School of Medicine (JHSOM). In study B, male Long Evans rats were exposed to  $^{16}\text{O}$  (1 GeV/n, 0.01–0.25 Gy) (16,19), and hearts were collected at 6–7 months and at 12 months after radiation. All heart samples from this study were shipped to UAMS and used for histology and western-blots.

### 2.1 Ethics statement

All animal procedures were approved by the Institutional Animal Care and Use Committees of UAMS, JHSOM, and Brookhaven National Laboratory (BNL).

### 2.2 Animal housing and radiation

In study A, 32 male Long Evans rats were obtained from Charles River (Wilmington, MA) at the age of 10 weeks and housed two per cage on a 12:12 hour light:dark cycle at UAMS. Rats received standard rodent chow low in soy (2020X, Harlan, Indianapolis, IN) and water *ad libitum* until they reached the age of 6 months. Starting at 21 weeks of age, all rats were rationed to 20 or 25 g chow per day, and the average rat weight was maintained within 620–750 g throughout the study. Two rats showed malocclusion, and their teeth were trimmed every few weeks throughout the study. At 6 months of age, rats were transported to BNL by overnight air (World Courier, New Hyde Park, NY) and housed 2 per cage on a 12:12 hour light:dark cycle, receiving 2020X rodent diet and water *ad libitum*. After 1 week acclimatization to BNL, rats were exposed to radiation at the NASA Space Radiation Laboratory (NSRL). Rats were placed in the NSRL beamline in a dark Plexiglas holder with two compartments, one rat per compartment. Rats received whole-body irradiation with a single dose of 0.5 Gy protons (250 MeV, 0.10–0.11 Gy/min,  $n=12$  rats), 0.5 Gy  $^{16}\text{O}$  (600 MeV/n, 0.10–0.11 Gy/min,  $n=10$  rats), or sham treatment (placement in the holder for the same amount of time as during radiation, but not placed in the beamline,  $n=10$  rats).

Radiation dosimetry was performed by the NSRL physicists. One day after irradiation, rats were returned to UAMS by overnight air and housed under the same conditions as described above.

Details of animal procedures in study B can also be found in Jones et al. (16) and Mange et al (19). Male Long Evans rats were obtained from Harlan Laboratories (Indianapolis, IN) and singly housed on a 12:12 hour light:dark cycle at JHSOM. Rats were maintained at 90% of their free-feeding weights by being fed measured amounts of chow. At 6 months of age, rats were transported to BNL and singly housed on a 12:12 hour light:dark cycle. After 4 days acclimatization to BNL, rats were exposed to radiation at NSRL. Rats were placed in the NSRL beamline in individual plastic holders and received whole-body irradiation with a single dose of 0.01, 0.05, 0.1 or 0.25 Gy  $^{16}\text{O}$  (1 GeV/n), or sham-irradiation. Radiation dosimetry was performed by the NSRL physicists. Ten days after irradiation, rats were returned to JHSOM and housed under the same conditions as described above. Rats exposed to 0 Gy (n=8 rats), 0.01 Gy (n=7 rats) and 0.1 Gy (n=8 rats) were followed up to 6 to 7 months after irradiation. Rats exposed to 0 Gy (n=5 rats), 0.05 Gy (n=8 rats) and 0.25 Gy (n=6 rats) were followed up to 12 months. During follow-up, these rats underwent testing to examine social odor recognition memory at one and 6 months after radiation. The methods and results of these tests are described by Jones et al. (16) and Mange et al. (19).

### 2.3 Ultrasonography

In study A, rats were assessed with ultrasonography at 3, 5, 9, and 12 months after irradiation. Of all methods of anesthesia, isoflurane inhalation is one of the approaches with the smallest effect on cardiac physiology (21). Nonetheless, a slowing of heart rate still occurs. Therefore, we developed a procedure in which rats were under anesthesia for the shortest possible time during ultrasonography, similar to our previous approach in the mouse (10). The day before each ultrasonography scan, rats were anesthetized with 2% isoflurane inhalation, and hair was removed from the thorax and abdomen using clippers and a depilatory cream. On the day of ultrasonography, rats were anesthetized with 1.5–2% isoflurane inhalation and immediately placed supine on a heated platform that monitors respiration rate and ECG. The rats were scanned with a Vevo® 2100 imaging system (VisualSonics, Toronto, Canada) and a MS250 (13–24 MHz) transducer. Echocardiographs were obtained in the short axis M-mode at the mid-left ventricular level. Pulsed-wave Doppler was used to determine mitral valve E and A velocities in a four-chamber view of the heart. Pulsed-wave Doppler was also used to measure blood flow velocity in the abdominal aorta. For this purpose, the probe was placed in the transverse axis, immediately anterior of the renal artery branch point. The Vevo® LAB cardiac and vascular software packages were used to obtain the parameters listed in Supplemental Material, Table S1.

### 2.4 Blood cell counts and blood chemistry values

In study A, at the time of sacrifice at 12 months after irradiation, all rats were anesthetized with 3% isoflurane inhalation and a drop of blood was drawn from a tail snip and used to measure blood glucose levels with a FreeStyle Precision Neo blood glucose monitoring system and test strips (Abbott Laboratories, Lake Bluff, IL). Then, an infusion set (25G, Becton Dickinson, Franklin Lakes, NJ) was placed in the abdominal vena cava and used to

inject a single dose of heparin (15 U/kg). Without changing the position of the infusion set, a blood sample was drawn and transferred into an EDTA coated tube for determination of circulating blood cell counts with a HEMAVET HV950 hemocytometer (Drew Scientific, Miami Lakes, FL) and blood chemistry values (listed in Supplemental Material, Table S2) with an i-STAT blood analyzer and CHEM8+ cartridges (Abbott Labs, Lake Bluff, IL).

## 2.5 Tissue collection

In study A, tissue was collected at 12 months after irradiation. After heparin injection and blood collection as described above, the heart was collected and within 10 minutes after collection of the heart, the abdominal aorta. The hearts were rinsed in PBS, weighed, and processed immediately upon removal. Hearts were cut into two longitudinal halves, and one half was fixed in 5% formalin for 24 hours and embedded in paraffin for histology. The other half was divided into atria, specimens of right ventricle, and specimens of left ventricle, snap-frozen and stored at  $-80^{\circ}\text{C}$ . The abdominal aorta was fixed in 5% formalin for 24 hours and embedded in paraffin for histology. Lastly, tibia length was measured as an indicator of body size.

In study B, rats were euthanized by decapitation at 6 to 7 months and at 12 months after irradiation. After collection of brain and blood for purposes beyond the current study, the heart was collected and cut into two longitudinal halves. One half was fixed in 5% formalin for 24 hours and embedded in paraffin for histology. The other half was snap-frozen and stored at  $-80^{\circ}\text{C}$ . All cardiac tissue samples were transported to UAMS for analysis.

## 2.6 Histology and immunohistochemistry

Five  $\mu\text{m}$  heart sections obtained in study A were stained with Hematoxylin and Eosin (H&E) and assessed by a veterinary pathologist (Stanley D. Kosanke, Heartland Veterinary Pathology Services, Edmond, OK) who was blinded for treatment group. Tissue sections were scored for acute inflammation, acute myofiber necrosis, microvascular damage, chronic interstitial fibrosis, and chronic epicardial fibrosis and were assessed for the presence of coronary artery and valvular damage.

Sections of abdominal aorta and heart were used to determine cardiac collagen deposition as previously described (22). Briefly, 5  $\mu\text{m}$  longitudinal sections of heart and 5  $\mu\text{m}$  transverse sections of aorta were rehydrated and incubated with Sirius Red supplemented with Fast Green. Sections were scanned with a ScanScope CS2 slide scanner and analyzed with ImageScope 12 software (Leica Biosystems, Wetzlar, Germany). The relative tissue area of collagens was calculated as the red-stained area expressed as a percentage of the total tissue area of each section.

For determination of mast cell numbers, sections were incubated in 0.5% Toluidine Blue in 0.5 N HCl for 3 days at room temperature, followed by 0.7 N HCl for 10 minutes. Eosin was used as a counterstain.

Immunohistochemistry was used to assess cardiac numbers of monocytes/macrophages. Antigen retrieval was performed by treating the sections with 10 mM sodium citrate (pH 6.0) at  $95^{\circ}\text{C}$  for 20 minutes. Sections were allowed to cool down prior to incubation in 1%

H<sub>2</sub>O<sub>2</sub> in methanol for 30 minutes to quench the endogenous peroxidase activity. Subsequently, sections were incubated overnight at 4°C with rabbit anti-CD68 (Santa Cruz Biotechnology, Santa Cruz, CA) diluted 1:200 in TBS, followed by biotinylated goat anti-rabbit IgG (1:200, Vector Laboratories, Burlingame, CA) for 90 minutes, an avidin-biotin-peroxidase complex (Vector Laboratories) for 45 minutes, and a solution of 0.5 mg/ml DAB (Sigma-Aldrich, St Louis, MO) and 0.003% H<sub>2</sub>O<sub>2</sub> in TBS for 5 minutes. Sections were counterstained with H&E.

Toluidine Blue, CardioTACS®, and anti-CD68 stained sections were examined with an Axioskop transmitted light microscope (Carl Zeiss, Oberkochen, Germany), and mast cells, apoptotic nuclei, and CD68-positive cells were counted and divided by the area of the tissue in each section. Counting was performed blinded for treatment group.

## 2.7 Western-blot analysis

A Potter-Elvehjem mechanical compact stirrer (BDC2002, Caframo, Georgian Bluffs, Canada) was used to homogenize left ventricular samples in a 1% Triton-X100 RIPA buffer containing 1:100 protease and phosphatase inhibitors (both Sigma-Aldrich). Protein concentration was determined using a BCA protein assay (Bio-Rad, Hercules, CA) and 25 µg protein was added to a 2x Laemmli buffer containing β-mercaptoethanol (5%). Gel electrophoresis was performed, and proteins were transferred overnight at 4°C to a PVDF membrane (all Bio-Rad). Membranes were incubated in TBS containing 0.05% Tween-20 and 5% non-fat dry milk to reduce non-specific antibody binding, followed by primary and secondary antibodies listed in Supplemental Material, Table S3 diluted in TBS containing 0.1% Tween-20 and 5% non-fat dry milk. Membranes were covered in ECL Plus Western Blotting Detection Reagent (GE Healthcare Life Sciences, Chicago, IL) and placed on CL-Xposure Film (Thermo Scientific, Waltham, MA). Films were developed and imaged with an AlphaImager® gel documentation system (ProteinSimple, San Jose, CA). Density of protein bands was determined with the publically available ImageJ software and expressed relative to GAPDH.

## 2.8 Statistics

Each ultrasonography parameter was first fitted with a repeated measures analysis of covariance comprised of radiation (an among-animal factor), time (a within-animal factor), and their interaction as factors, and time-specific heart rate as a covariate. Heart rate during ultrasonography recording was included as covariate since it is known that echocardiography outcomes may depend on heart rate (21). Regarding the repeated measures, the lowest (best) Bayesian Information Criterion was used to choose the within-animal covariance from among these structures: exchangeable, autoregressive, Toeplitz, or general. Denominator degrees of freedom were estimated with Kenward-Roger's method.

All other parameters were fitted with an analysis of variance with radiation, time, and the radiation × time interaction as (among-animal) factors. In each analysis, the radiation groups were compared to the sham group within the same time point.

For all analyses, residuals were checked for adherence to the normal assumption via visual inspection of Q-Q plots, and for adherence to homogeneous variance with Levene's test. In

all instances, normal assumptions were reasonable. For some parameters, though, variances were not homogeneous; in those cases, we allowed for heterogeneous variance through the covariance structure of the model. All tests were conducted at a 0.05 significance level. Analyses were conducted with the MIXED procedure in SAS/STAT software, version 9.4 (SAS System for Windows, SAS Institute, Inc.). Because the purpose of the study was to identify potential heart measures for future study, no adjustment for multiple comparisons were applied.

### 3. Results

#### 3.1 Results study A

In study A, male Long Evans rats were exposed to protons (250 MeV) or  $^{16}\text{O}$  (600 MeV/n), transported to UAMS and housed for 12 months after irradiation. Ultrasonography was used to measure *in vivo* cardiac function and blood flow parameters, and at 12 months, circulating blood cells were counted, blood chemistry was measured, and heart and abdominal aorta were collected for histology and western-blot. The research results are described in sections 3.1.1 – 3.1.5.

**3.1.1 Animal characteristics**—At 12 months after radiation, no changes were observed in heart weight or heart weight relative to tibia length (to correct for body size, Supplemental Material, Table S4). In addition, no changes were observed in circulating blood cell counts (Table 1), or blood chemistry values at 12 months (Supplemental Material, Table S5).

**3.1.2 Ultrasonography**—Ultrasonography results obtained at 3–12 months after radiation are presented in Table 2 (systolic function parameters) and Supplemental Material, Tables S6 (ventricular dimensions) and S7 (Power Doppler measurements in abdominal aorta). Small but significant decreases were found in left ventricular posterior wall thickness at 3 and 5 months after protons and  $^{16}\text{O}$ . In addition, cardiac volume at the end of systole was increased in proton exposed rats compared to sham controls at all time points and reached statistical significance at 3 and 9 months. At 12 months, none of the measurements of cardiac dimensions or function were altered by radiation. On the other hand, in assessment of the abdominal aorta, an increase was seen in mean velocity, peak velocity, and velocity time integral at 12 months after  $^{16}\text{O}$  (Supplemental Material, Table S7), suggesting a change in vascular function at this late post-radiation time point.

**3.1.3 Histopathology**—Sections of hearts obtained at 12 months after radiation were assessed for the presence of histopathological changes. All histopathological assessments are presented in Supplemental Material, Table S8. In summary, none of the hearts showed signs of inflammation, myofiber necrosis, microvascular damage, or epicardial fibrosis. Very mild to mild, focal to multifocal evidence of interstitial fibrosis was observed in 3 out of 10 sham-irradiated rats, 4 out of 12 proton-exposed rats, and 3 out of 10  $^{16}\text{O}$ -exposed rats (Table 3). Since these changes were seen in rats of all three groups, including sham-irradiated controls, they were most likely due to aging.

**3.1.4 Extracellular matrix remodeling**—Histological staining was performed to determine total collagen deposition in the heart and wall of abdominal aorta. Quantitative image analysis showed that protons (250 MeV) or  $^{16}\text{O}$  (600 MeV/n) did not alter the cardiac tissue area occupied by total collagens (Supplemental Material, Figure S1). Similarly, transverse sections of abdominal aorta from the same animals did not show a change in percentage of tissue occupied by collagen (data not shown).

The rat and human heart contain low numbers of mast cells (23,24). In previous studies with high-dose local X-ray exposure of the heart in rodent models, we found a strong correlation between cardiac mast cell numbers and collagen deposition (25). Therefore, we assessed cardiac mast cell numbers and cardiac tissue protein levels of mast cell tryptase as potential indicators of radiation-induced tissue remodeling. Exposure to protons (250 MeV) or  $^{16}\text{O}$  (600 MeV/n) did not change cardiac mast cell numbers or left ventricular protein levels of mast cell tryptase (Supplemental Material, Figure S2). Toluidine Blue staining did not detect any mast cells in the aorta wall (data not shown).

Lastly, we assessed collagen type III, the most abundant collagen type in the heart, with western-blot. Rat collagen type III is about 300 kDa in size. However, we detected a collagen type III protein band of approximately 75 kDa. This appears to be a truncated peptide of collagen type III that we have previously described in western-blot analysis of the mouse heart (10, 11). The tissue content of the 75 kDa collagen type III peptide was significantly increased in samples of the left ventricle at 12 months after protons (250 MeV) (Figure 1).

**3.1.5 Cardiac immune cells**—Western-blot analysis was used to assess protein levels of the general T-lymphocyte marker CD2, and markers of T-helper cells and cytotoxic T-cells, CD4 and CD8, respectively. Exposure to  $^{16}\text{O}$  (600 MeV/n) caused an increase in protein levels of CD2 (Figure 2), CD4 and CD8 (Supplemental Material, Figure S3).

In addition,  $^{16}\text{O}$  (600 MeV/n) caused an increase in protein levels of CD68. However, immunohistochemical analysis revealed no significant change in the number of CD68-positive cells in the heart (Figure 3).

## 3.2 Results study B

Study B was part of a tissue sharing approach, in which hearts were obtained from male Long Evans rats that were exposed to  $^{16}\text{O}$  (1 GeV/n) at doses from 0.01 to 0.25 Gy and housed at JHSOM (16,19). Hearts were collected at 6–7 months and at 12 months after radiation, and the results of heart tissue analysis are described below.

Quantitative image analysis showed that  $^{16}\text{O}$  (1 GeV/n) did not alter the cardiac tissue area occupied by total collagens (Supplemental Material, Figure S4). On the other hand, the tissue content of the 75 kDa collagen type III peptide that was also observed in study A (see section 3.1.4), was significantly increased at 12 months after  $^{16}\text{O}$  (1 GeV/n) at doses of 0.05 and 0.25 Gy (Supplemental Material, Figure S5). While  $^{16}\text{O}$  caused an increase in cardiac protein levels of mast cell tryptase at all doses examined, there was no increase in cardiac numbers of mast cells (Supplemental Material, Figure S6).



An increase was observed in protein levels of T-lymphocyte marker CD2 after exposure to  $^{16}\text{O}$  at doses of 0.05 Gy and above (Supplemental Material, Figure S7). The cardiac protein levels of CD4 and CD8 were increased only at 6 months after a dose of 0.1 Gy (Supplemental Material, Figure S8). Lastly, while CD68 protein levels were also increased at doses of 0.05 Gy and above, numbers of CD68 positive cells as determined with immunohistochemistry were not altered by radiation (Supplemental Material, Figure S9).

#### 4. Discussion

Preclinical research performed in multiple animal species may enhance the translatability of the results to human subjects. While most studies of cardiovascular effects of space radiation have been performed in mouse models (9–12), studies in the rat could provide input from a second animal species. We performed ultrasonography in male Long Evans rats exposed to protons (250 MeV) or  $^{16}\text{O}$  (600 MeV/n) at a dose of 0.5 Gy. While there were some small changes in left ventricular wall thickness and volume, no changes were seen in ultrasonography measures that indicate systolic function (such as ejection fraction) or diastolic function (mitral valve E/A velocity ratios). On the other hand, in a previous study by Soucy et al, exposure of male Wistar rats to a dose of 1 Gy  $^{56}\text{Fe}$  (1 GeV/n), but not to 0.5 Gy, caused an increase in abdominal aorta pulsed-wave velocity when measured at 8 months after irradiation (15). Together with other *in vivo* and *ex vivo* measures of vascular function, the authors concluded that exposure to  $^{56}\text{Fe}$  caused a xanthine oxidase-dependent vascular dysfunction. In the current study, protons did not cause changes in pulsed-wave velocity in the abdominal aorta, but  $^{16}\text{O}$  at a dose of 0.5 Gy caused an increase in mean velocity, peak velocity and velocity time integral at 12 months after irradiation. Altogether, ultrasonography results suggest that  $^{16}\text{O}$ , while not inducing changes in cardiac function, may cause long-term vascular dysfunction in the rat, similar to the findings by Soucy et al on  $^{56}\text{Fe}$  (15).

In addition to cardiovascular function, we examined effects of protons and  $^{16}\text{O}$  on tissue structure. For this purpose, we made use of samples from two studies. In study A, samples of heart and abdominal aorta were collected from Long Evans rats exposed to protons (250 MeV) or  $^{16}\text{O}$  (600 MeV/n) at a dose of 0.5 Gy, also described in the ultrasonography studies above. In study B, hearts were obtained from Long Evans rats exposed to  $^{16}\text{O}$  (1 GeV/n, 0.01 – 0.25 Gy) (16,19). There were some differences in the design of the two studies.  $^{16}\text{O}$  was administered at different energies and radiation doses, and there were differences in environmental factors such as housing and diet. In addition, during follow-up in study B, the rats underwent testing to examine social odor recognition memory, as part of a separate neurocognitive study, at one and 6 months after radiation (16,19). Moreover, tissue samples in studies A and B were collected at different time points after irradiation. Lastly, in study A, samples of left ventricle were used for western-blots, while in study B only samples of whole heart that may have contained small amounts of right ventricular and atrial tissue were available. This may have an effect on western-blot outcome if the expression of a protein depends on its anatomical location in the heart. However, since all tissue endpoints were compared with age-, time-, and institution-matched sham-irradiated controls within each of the studies, we believe that results of both studies will be useful in obtaining insight into effects of low-dose  $^{16}\text{O}$  exposures on the heart.

We found no increase in total tissue area occupied by collagens in cardiac sections of the two studies. On the other hand, we did observe an increase in tissue content of a 75 kDa collagen type III peptide in the left ventricle at 12 months after protons (250 MeV, 0.5 Gy) and in samples of the whole heart at 12 months after  $^{16}\text{O}$  (1 GeV/n) at doses of 0.05 and 0.25 Gy. We have previously shown an increase in this peptide of collagen type III in samples of whole heart of male C57BL/6 mice at 7 days after whole-body exposure to  $^{56}\text{Fe}$  (600 MeV/n, 0.5 Gy) (11) and in samples of left ventricle of male C57BL/6J mice at 2 weeks, 3 months and 9 months after protons (150 MeV, 1 Gy) and  $^{16}\text{O}$  (600 MeV/n, 1 Gy) (10). We believe that this is a truncated form of collagen type III that is indicative of a remodeling process of this collagen. Recently, it has been shown that peptide fragments of collagens due to extracellular matrix remodeling play an active role in regulating cellular processes such as cell death and angiogenesis (26,27). Together, the results in mice and rats suggest that while radiation fibrosis does not occur after low doses of protons or high-energy heavy ions, these forms of radiation do induce the remodeling of existing collagens in the heart.

We examined left ventricular and whole heart protein content of T-lymphocyte markers CD2, CD4 and CD8. All three T-lymphocyte markers were increased at 6 months after  $^{16}\text{O}$  (1 GeV/n) at a dose of 0.1 Gy and 12 months after  $^{16}\text{O}$  (600 MeV/n) at a dose of 0.5 Gy. Left ventricular and whole heart protein levels of the monocyte/macrophage marker CD68 were increased in the same radiation groups. However, immunohistochemistry did not reveal a change in the number of CD68 positive cells in the heart. In addition, while there was an increase in cardiac protein levels of mast cell tryptase at 6 to 7 months and at 12 months after  $^{16}\text{O}$  at an energy of 1 GeV/n, histological staining did not reveal an increase in cardiac numbers of mast cells. In future studies, it may be important to incorporate more sensitive methods to determine immune cell numbers, such as flow cytometry of freshly obtained cardiac tissue samples, to obtain a definite answer on immune cell infiltration in the heart.

Cardiac remodeling after high-dose whole-body irradiation has been shown to depend on kidney function (28,29). We assessed a panel of biochemical indicators of kidney function at 12 months after irradiation in study A and found no alterations. Therefore, it is not likely that radiation-induced alterations observed in the heart were an indirect effect of radiation effects on the kidney. Additional pathophysiological measurements are required to further assess the long-term biological consequences of low-dose space radiation on the rat cardiovascular system.

The radiation doses tested in studies A and B were relevant for total doses received during deep-space missions. However, practical considerations limited us to administering these radiation doses within several minutes, while the dose rates of charged particle exposure during space travel are many fold lower (30). Further studies need to determine the effects of mixed ion fields and protracted radiation exposures in both male and female animals. Moreover, even if certain findings are observed in two separate animal species, they may not always translate to human subjects (31). In terms of normal tissue radiation effects, for instance, differences in radiation sensitivity between species may complicate the assessment of biological response to specific radiation doses (32).

In conclusion, these studies did not reveal significant changes in cardiac function or cardiac histopathology in a rat model of single-dose whole body exposures to protons or  $^{16}\text{O}$ . However, some indications of mild changes in vascular function and remodeling of existing collagens in the heart were seen. These studies corroborate most of the findings previously obtained from mouse models of exposure to single doses of high-LET single ion radiation.

## Supplementary Material

Refer to Web version on PubMed Central for supplementary material.

## Acknowledgements

This work was supported by the National Space Biomedical Research Institute through NCC 9-58 under grants RE03701 [M.B.], PF02602 [C.M.D.] and NBP02802 [C.M.D.], NASA grants NNX15AC71G [C.M.D.], 80NSSC18K1080 [C.M.D.], 80NSSC17K0425 [M.B.], and 80NSSC19K0437 [M.B.], and NIGMS grant P20 GM109005 [M.B.]. The authors wish to thank the BNL support group, the NSRL physicists, the UAMS Experimental Pathology Core, and the animal care staff at UAMS, JHSOM and BNL for their excellent technical support.

## References

- Ozasa K, Takahashi I, Grant EJ, Kodama K. Cardiovascular disease among atomic bomb survivors. *Int J Radiat Biol* 2017;93(10):1145–1150. [PubMed: 28151038]
- Preston DL, Shimizu Y, Pierce DA, Suyama A, Mabuchi K. Studies of mortality of atomic bomb survivors. Report 13: Solid cancer and noncancer disease mortality: 1950–1997. *Radiat Res* 2003;160(4):381–407. [PubMed: 12968934]
- Carr ZA, Land CE, Kleinerman RA, Weinstock RW, Stovall M, Griem ML, Mabuchi K. Coronary heart disease after radiotherapy for peptic ulcer disease. *Int J Radiat Oncol Biol Phys* 2005;61(3):842–50. [PubMed: 15708264]
- Ivanov VK, Maksioutov MA, Chekin SY, Petrov AV, Biryukov AP, Kruglova ZG, Matyash VA, Tsyb AF, Manton KG, Kravchenko JS. The risk of radiation-induced cerebrovascular disease in Chernobyl emergency workers. *Health Phys* 2006;90(3):199–207. [PubMed: 16505616]
- Little MP, Azizova TV, Bazyka D, Bouffler SD, Cardis E, Chekin S, Chumak VV, Cucinotta FA, de VF, Hall P, Harrison JD, Hildebrandt G, Ivanov V, Kashcheev VV, Klymenko SV, Kreuzer M, Laurent O, Ozasa K, Schneider T, Tapio S, Taylor AM, Tzoulaki I, Vandoolaeghe WL, Wakeford R, Zablotzka LB, Zhang W, Lipshultz SE. Systematic review and meta-analysis of circulatory disease from exposure to low-level ionizing radiation and estimates of potential population mortality risks. *Environ Health Perspect* 2012;120(11):1503–11. [PubMed: 22728254]
- Cucinotta FA, Durante M. Cancer risk from exposure to galactic cosmic rays: implications for space exploration by human beings. *Lancet Oncol* 2006;7(5):431–5. [PubMed: 16648048]
- Zeitlin C, Hassler DM, Cucinotta FA, Ehresmann B, Wimmer-Schweingruber RF, Brinza DE, Kang S, Weigle G, Böttcher S, Böhm E, Burmeister S, Guo J, Köhler J, Martin C, Posner A, Rafkin S, Reitz G. *Science* 2013;340(6136):1080–4. [PubMed: 23723233]
- Hassler DM, Zeitlin C, Wimmer-Schweingruber RF, Ehresmann B, Rafkin S, Eigenbrode JL, Brinza DE, Weigle G, Böttcher S, Böhm E, Burmeister S, Guo J, Köhler J, Martin C, Reitz G, Cucinotta FA, Kim MH, Grinspoon D, Bullock MA, Posner A, Gómez-Elvira J, Vasavada A, Grotzinger JP; MSL Science Team. *Science* 2014;343(6169):1244797. [PubMed: 24324275]
- Yan X, Sasi SP, Gee H, Lee J, Yang Y, Mehrzad R, Onufrak J, Song J, Enderling H, Agarwal A, Rahimi L, Morgan J, Wilson PF, Carrozza J, Walsh K, Kishore R, Goukassian DA. Cardiovascular risks associated with low dose ionizing particle radiation. *PLoS One* 2014;9(10):e110269. [PubMed: 25337914]
- Seawright JW, Sridharan V, Landes RD, Cao M, Singh P, Koturbash I, Mao XW, Miousse IR, Singh SP, Nelson GA, Hauer-Jensen M, Boerma M. Effects of low-dose oxygen ions and protons on cardiac function and structure in male C57BL/6J mice. *Life Sci Space Res* 2019;20:72–84.

11. Ramadan SS, Sridharan V, Koturbash I, Miousse IR, Hauer-Jensen M, Nelson GA, Boerma M. A priming dose of protons alters the early cardiac cellular and molecular response to <sup>56</sup>Fe irradiation. *Life Sci Space Res (Amst)* 2016;8:8–13. [PubMed: 26948008]
12. Tungjai M, Whorton EB, Rithidech KN. Persistence of apoptosis and inflammatory responses in the heart and bone marrow of mice following whole-body exposure to 28Silicon (28Si) ions. *Radiat Environ Biophys* 2013;52(3):339–50. [PubMed: 23756637]
13. Coleman MA, Sasi SP, Onufrak J, Natarajan M, Manickam K, Schwab J, Muralidharan S, Peterson LE, Alekseyev YO, Yan X, Goukassian DA. Low-dose radiation affects cardiac physiology: gene networks and molecular signaling in cardiomyocytes. *Am J Physiol Heart Circ Physiol* 2015;309(11):H1947–H1963. [PubMed: 26408534]
14. Beheshti A, McDonald JT, Miller J, Grabham P, Costes SV. GeneLab Database Analyses Suggest Long-Term Impact of Space Radiation on the Cardiovascular System by the Activation of FYN Through Reactive Oxygen Species. *Int J Mol Sci.* 2019;20(3).
15. Soucy KG, Lim HK, Kim JH, Oh Y, Attarzadeh DO, Sevinc B, Kuo MM, Shoukas AA, Vazquez ME, Berkowitz DE. HZE (5)(6)Fe-ion irradiation induces endothelial dysfunction in rat aorta: role of xanthine oxidase. *Radiat Res* 2011;176(4):474–85. [PubMed: 21787183]
16. Jones CB, Mange A, Granata L, Johnson B, Hienz RD, Davis CM. Short and Long-Term Changes in Social Odor Recognition and Plasma Cytokine Levels Following Oxygen (16O) Ion Radiation Exposure. *Int J Mol Sci* 2019;20(2).
17. Johnson D, Lawrence SE, Livingston EW, Hienz RD, Davis CM, Lau AG. Modeling Space Radiation Induced Bone Changes in Rat Femurs through Finite Element Analysis. *Conf Proc IEEE Eng Med Biol Soc* 2018;2018:1763–6. [PubMed: 30440736]
18. Davis CM, DeCicco-Skinner KL, Roma PG, Hienz RD. Individual differences in attentional deficits and dopaminergic protein levels following exposure to proton radiation. *Radiat Res* 2014;181:258–71. [PubMed: 24611657]
19. Mange A, Cao Y, Zhang S, Hienz RD, Davis CM. Whole-Body Oxygen ((16)O) Ion-Exposure-Induced Impairments in Social Odor Recognition Memory in Rats are Dose and Time Dependent. *Radiat Res* 2018;189(3):292–9. [PubMed: 29332539]
20. Walker SA, Townsend LW, Norbury JW. Heavy ion contributions to organ dose equivalent for the 1977 galactic cosmic ray spectrum. *Adv Space Res* 2013;51:1792–9.
21. Wu J, Bu L, Gong H, Jiang G, Li L, Ma H, Zhou N, Lin L, Chen Z, Ye Y, Niu Y, Sun A, Ge J, Zou Y. Effects of heart rate and anesthetic timing on high-resolution echocardiographic assessment under isoflurane anesthesia in mice. *J Ultrasound Med* 2010;29(12):1771–8. [PubMed: 21098849]
22. Sridharan V, Seawright JW, Antonawich FJ, Garnett M, Cao M, Singh P, Boerma M. Late Administration of a Palladium Lipoic Acid Complex (POLY-MVA) Modifies Cardiac Mitochondria but Not Functional or Structural Manifestations of Radiation-Induced Heart Disease in a Rat Model. *Radiat Res* 2017;187(3):361–6. [PubMed: 28231026]
23. Hellstrom B, Holmgren H. Numerical distribution of mast cells in the human skin and heart. *Acta Anat (Basel)* 1950;10(1–2):81–107. [PubMed: 14777248]
24. Constantinides P, Rutherford J. Effects of age and endocrines on the mast cell counts of the rat myocardium. *J Gerontol* 1957;12(3):264–9. [PubMed: 13463295]
25. Boerma M, Zurcher C, Esveldt I, Schutte-Bart CI, Wondergem J. Histopathology of ventricles, coronary arteries and mast cell accumulation in transverse and longitudinal sections of the rat heart after irradiation. *Oncol Rep* 2004;12:213–9. [PubMed: 15254680]
26. Gaggari A, Weathington N. Bioactive extracellular matrix fragments in lung health and disease. *J Clin Invest.* 2016;126(9):3176–84. [PubMed: 27584731]
27. Kisling A, Lust RM, Katwa LC. What is the role of peptide fragments of collagen I and IV in health and disease? *Life Sci.* 2019;228:30–34. [PubMed: 31004660]
28. Lenarczyk M, Lam V, Jensen E, Fish BL, Su J, Koprowski S, Komorowski RA, Harmann L, Migrino RQ, Li XA, Hopewell JW, Moulder JE, Baker JE. Cardiac injury after 10 Gy total body irradiation: indirect role of effects on abdominal organs. *Radiat Res* 2013;180(3):247–58. [PubMed: 23919311]
29. Adams MJ, Grant EJ, Kodama K, Shimizu Y, Kasagi F, Suyama A, Sakata R, Akahoshi M. Radiation dose associated with renal failure mortality: a potential pathway to partially explain

- increased cardiovascular disease mortality observed after whole-body irradiation. *Radiat Res* 2012;177(2):220–8. [PubMed: 22149958]
30. Cucinotta FA, Wu H, Shavers MR, George K. Radiation dosimetry and biophysical models of space radiation effects. *Gravit Space Biol Bull* 2003;16(2):11–8. [PubMed: 12959127]
  31. Pound P, Ritskes-Hoitinga M. Is it possible to overcome issues of external validity in preclinical animal research? Why most animal models are bound to fail. *J Transl Med*. 2018;16(1):304. [PubMed: 30404629]
  32. MacVittie TJ, Farese AM, Kane MA. ARS, DEARE, and Multiple-organ Injury: A Strategic and Tactical Approach to Link Radiation Effects, Animal Models, Medical Countermeasures, and Biomarker Development to Predict Clinical Outcome. *Health Phys*. 2019;116(3):297–304. [PubMed: 30608246]

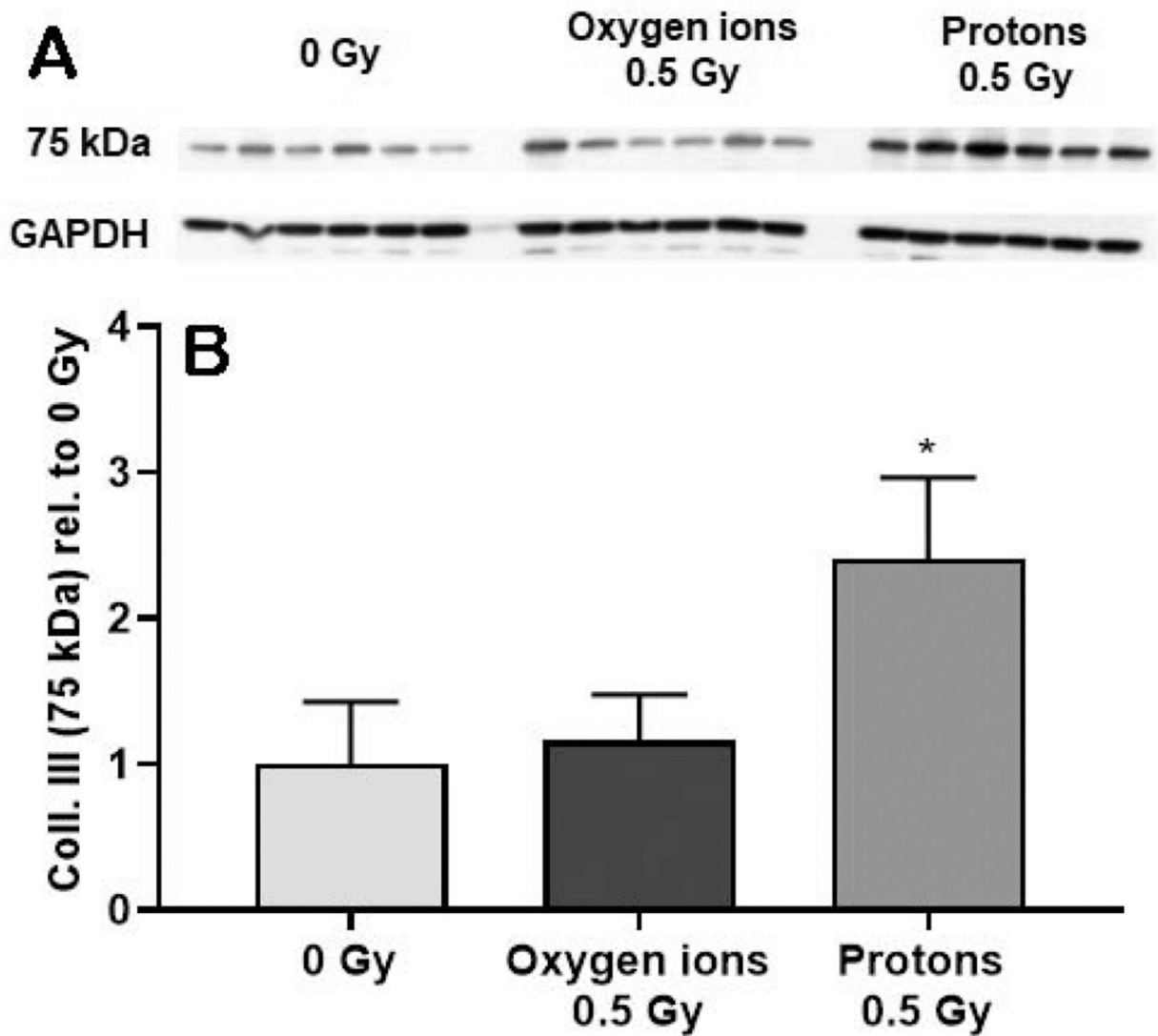


**Figure 1. Western-blot analysis of collagen type III (Coll. III) in the left ventricle.** Western-blot analysis revealed a 75 kDa peptide of collagen type III (A). The levels of this collagen type III peptide were quantified, normalized to GAPDH and then calculated relative to age- and time-matched 0 Gy controls (B). Samples of left ventricle were assessed at 12 months after oxygen ions (600 MeV/n) and protons (250 MeV),  $n=8$  rats in 0 Gy and  $n=10-12$  rats in the 0.5 Gy groups. Bars indicate average and SD. \* $p < 0.05$  compared to age- and time-matched 0 Gy.

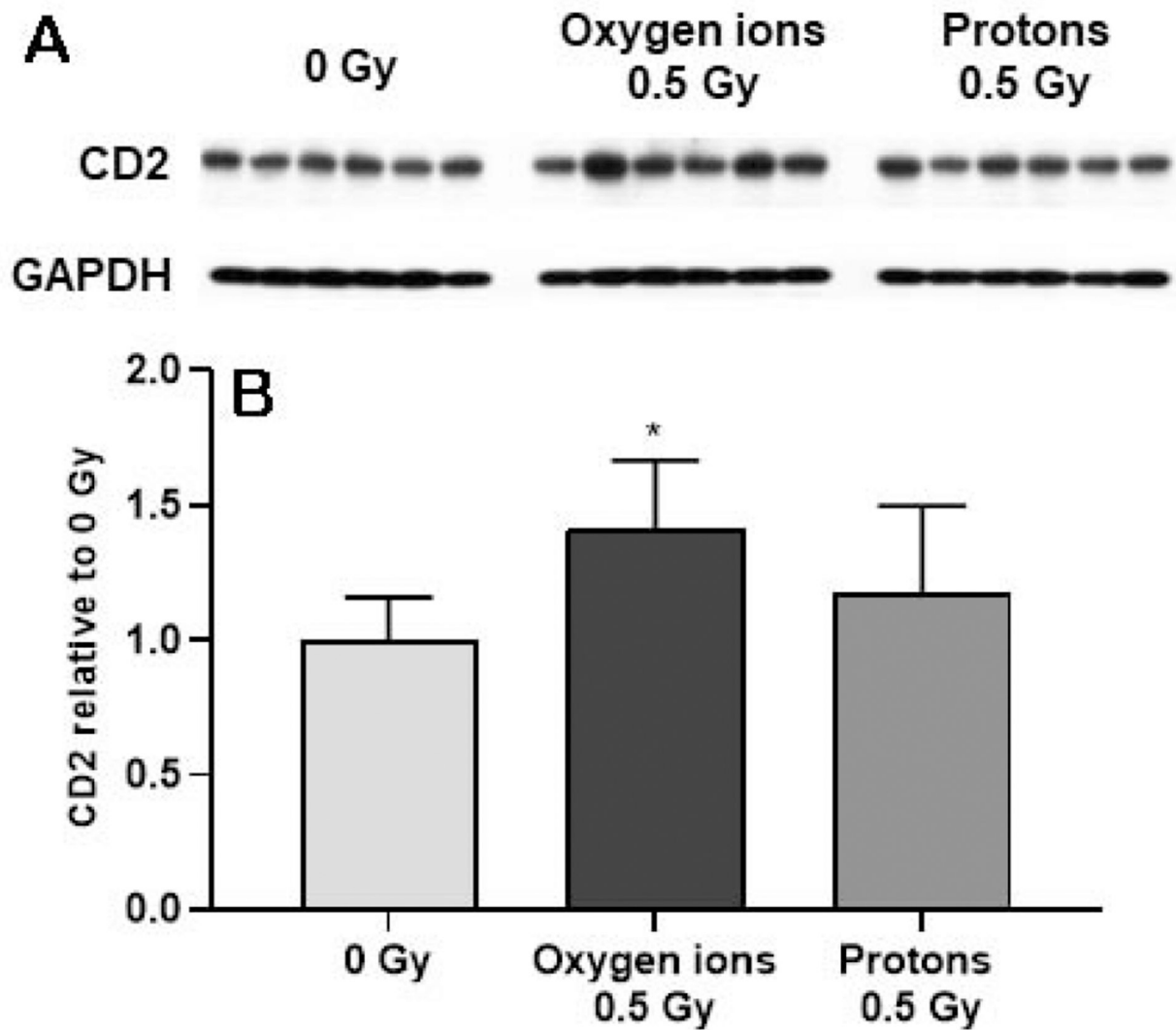


**Figure 2. Western-blot analysis of CD2 in the left ventricle.**

The levels of CD2 were quantified (A), normalized to GAPDH and then calculated relative to age- and time-matched 0 Gy controls (B). Samples of left ventricle were assessed at 12 months after oxygen ions (600 MeV/n) and protons (250 MeV),  $n=8$  rats in 0 Gy and  $n=10-12$  rats in the 0.5 Gy groups. Bars indicate average and SD. \* $p < 0.05$  compared to age- and time-matched 0 Gy.

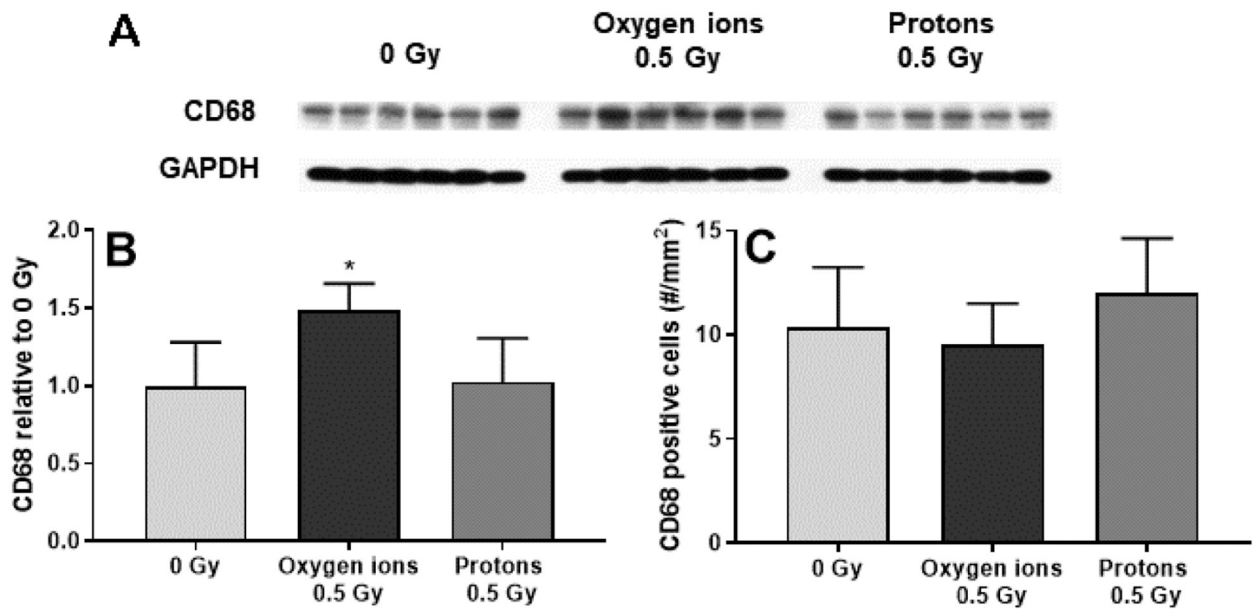


**Figure 3. Western-blot and immunohistochemical analysis of CD68 in the left ventricle.** Western-blot analysis was used to assess protein levels of CD68 (A), normalized to GAPDH and then calculated relative to age- and time-matched 0 Gy controls (B). Immunohistochemistry was used to determine the number of CD68-positive cells per mm<sup>2</sup> of cardiac tissue area (C). CD68-positive cells and left ventricular CD68 protein levels were assessed at 12 months after protons (250 MeV) and oxygen ions (600 MeV/n),  $n=8$  rats in 0 Gy and  $n=10-12$  rats in the 0.5 Gy groups. Bars indicate average and SD. \* $p < 0.05$  compared to time-matched 0 Gy.



**Table 1.**

Circulating blood cell counts at 12 months after radiation

Parameter	0 Gy	<sup>16</sup> O (0.5 Gy)	Protons (0.5 Gy)
White blood cells (*10 <sup>3</sup> /μl)	3.42 ± 1.81	2.61 ± 1.01	4.14 ± 6.32
Neutrophils (%)	44.4 ± 12.1	48.8 ± 10.1	42.9 ± 14.6
Lymphocytes (%)	47.9 ± 13.4	43.4 ± 9.2	51.6 ± 14.1
Monocytes (%)	6.4 ± 3.1	6.9 ± 3.1	4.5 ± 1.7
Eosinophils (%)	1.0 ± 0.5	0.9 ± 0.6	1.1 ± 1.0
Basophils (%)	0.2 ± 0.1	0.1 ± 0.2	0.1 ± 0.2
Red blood cells (*10 <sup>6</sup> /μl)	6.55 ± 1.01	7.59 ± 1.06	6.14 ± 1.71

Values indicate average ± SD, *n*=10–12 rats per group. In all statistical comparisons in the manuscript, the radiation groups were compared with age-matched sham controls. There were no statistically significant differences between the groups.

Author Manuscript

Author Manuscript

Author Manuscript

Author Manuscript

**Table 2.**

Results of cardiac ultrasound after sham-irradiation (0 Gy) and exposure to protons (250 MeV, 0.5 Gy) or  $^{16}\text{O}$  (600 MeV/n, 0.5 Gy)

Parameter		3 months	5 months	9 months	12 months
sv ( $\mu\text{l}$ )	0 Gy	301.2 $\pm$ 81.8	258.2 $\pm$ 57.2	292.3 $\pm$ 49.6	306.7 $\pm$ 55.9
	$^{16}\text{O}$	304.8 $\pm$ 31.4	289.1 $\pm$ 27.1	308.7 $\pm$ 27.6	315.6 $\pm$ 36.3
	Protons	294.3 $\pm$ 27.3	284.0 $\pm$ 50.2	293.5 $\pm$ 34.6	314.0 $\pm$ 33.5
EF (%)	0 Gy	76.5 $\pm$ 6.4	74.1 $\pm$ 3.9	80.0 $\pm$ 6.0	79.9 $\pm$ 7.6
	$^{16}\text{O}$	75.6 $\pm$ 4.9	74.8 $\pm$ 5.1	76.4 $\pm$ 5.4	76.6 $\pm$ 3.7
	Protons	72.1 $\pm$ 7.2	76.7 $\pm$ 4.9	75.3 $\pm$ 8.5	76.7 $\pm$ 4.7
FS (%)	0 Gy	47.4 $\pm$ 5.9	44.8 $\pm$ 3.9	50.9 $\pm$ 6.4	51.3 $\pm$ 8.3
	$^{16}\text{O}$	46.4 $\pm$ 4.5	45.7 $\pm$ 4.6	47.3 $\pm$ 5.3	47.4 $\pm$ 3.6
	Protons	43.5 $\pm$ 6.5	47.4 $\pm$ 4.4	46.5 $\pm$ 8.1	47.5 $\pm$ 4.6
CO (ml/min)	0 Gy	111.4 $\pm$ 30.5	95.5 $\pm$ 24.4	104.1 $\pm$ 18.4	107.4 $\pm$ 21.8
	$^{16}\text{O}$	108.8 $\pm$ 11.0	100.8 $\pm$ 11.2	100.4 $\pm$ 16.8	127.3 $\pm$ 54.8
	Protons	103.2 $\pm$ 7.9	115.7 $\pm$ 35.1	112.0 $\pm$ 33.9	112.1 $\pm$ 12.1

Values indicate average  $\pm$  SD,  $n=8$  rats in 0 Gy and  $n=10-12$  rats in the 0.5 Gy groups. There were no significant differences between the radiation groups and time-matched 0 Gy controls. Additional cardiac ultrasound parameters are presented in Supplemental Material, Table S6.

**Table 3.**

Histopathological scoring of interstitial fibrosis at 12 months after exposure to  $^{16}\text{O}$  (600 MeV/n, 0.5 Gy) or protons (250 MeV, 0.5 Gy)

Dose group	Scores of individual rats
0 Gy	0, 0, 0, 0, 0, 0, 0, 1, 1, 1
$^{16}\text{O}$ (0.5 Gy)	0, 0, 0, 0, 0, 0, 0, 0.5, 1, 1
Protons (0.5 Gy)	0, 0, 0, 0, 0, 0, 0, 0, 0.5, 0.5, 0.5, 1

Longitudinal sections of heart were scored for interstitial fibrosis using the following grading system: 0 = no lesions; 0.5–1 = mild changes; 1.5–2 = moderate changes; 2.5–3 = marked changes; 3.5–4 = severe changes.

Author Manuscript

Author Manuscript

Author Manuscript

Author Manuscript